

## Simulation of Meteoroid Impact Effects

on

### Expandable Structures

1/Lt. Andre J. Holten

#### INTRODUCTION

The micrometeoroid simulation facility, located at WPAFB, was developed to fulfill the needs for materials testing within the AF Materials Laboratory as well as a support to other organizations with requirements for hypervelocity impact data. The technique used for the acceleration of the milligram size particles is the exploding foil device.

The AFML hypervelocity<sup>(1)</sup> facility consists of an electronically-triggered, high-energy storage system together with high-speed streak and framing photographic instrumentation for measuring particle velocity, size, shape, and momentum. Electronic instrumentation is provided for measuring capacitor bank discharge characteristics and the energy input to the exploding-foil fun.

Since the gun disintegrates when it is fired, a special room houses the evacuated gun chamber and exploding-foil gun to protect equipment and operating personnel. Also provided is a shielded control room, a dark room, and a data analysis area.

#### THE AIR FORCE MATERIALS LABORATORY EXPLODING FOIL FACILITY

##### Energy Storage System

The energy storage system consists of four banks of capacitors (Cornell-Cublier Type NRG 381), with each bank

# Contracts

composed of ten  $1\text{-}\mu\text{F}$ , 100-kV capacitors connected in parallel. At full rated voltage, the capacitors store 5000 J each, providing a total stored energy of 2000,000 J. At this energy level, however, the manufacturer guarantees the capacitors for only 1000 shots. If the capacitors are charged to no more than 50 kV, the guarantee is extended to 10,000 shots or 1 year. Because many more than 1000 shots are to be fired, it was agreed that the bank be given a rating of 50 kV maximum with a corresponding stored energy of 50,000 J.

The radial arrangement of the banks (Figure 1) was chosen to minimize the length of the discharge cables connecting the banks to the exploding-foil gun. Each bank is discharged through a three electrode reduced pressure trigger gap switch. The pressure is chosen such that jitter is minimized on firing at a particular voltage. At the correct pressure all four switches fire within  $0.05\ \mu\text{sec}$ . of each other. The total circuit inductance is 92.1 nanohenries. The total circuit ring frequency is 80 kc. The gun contributes nominal inductance to the circuit with the result that the circuit firing conditions are rather independent of the gun design. The discharge conditions at the full rated voltage of 50,000 V are:

Peak current  $7 \times 10^5$  amps  
Energy delivered during first half  
cycle 15,000 J  
Time to peak current  $3\ \mu\text{sec}$ .  
Half width of initial power pulse  $2\ \mu\text{sec}$ .

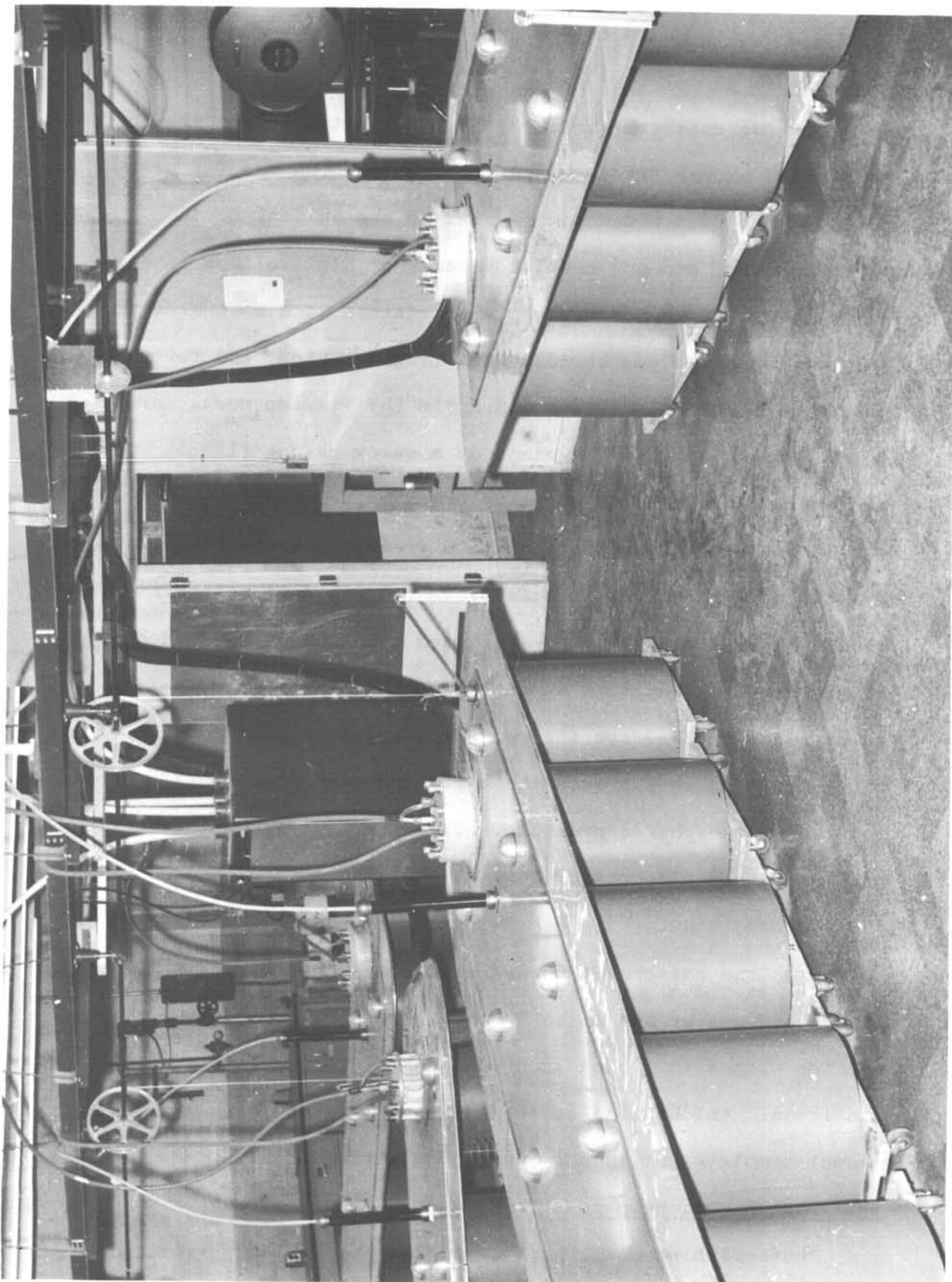


Figure 1. Overall View of the AFML Facility

## Gun Chamber

The gun chamber (Figure 2) is constructed from a standard 3-in. cast bronze "cross" pipe fitting to which special brass flanges have been added for supporting the optical ports, target holder, and gun mount. Because of high-voltage insulation problems, the gun breech is maintained at atmospheric pressure and only the gun barrel, free-flight region, and target are evacuated. Optical flats are used in the viewing ports and are held in place against "O" rings by a quick-change flange. The diameter of the viewing ports is 6 cm.

The chamber provides a maximum free-flight distance of 25 cm. A modified Kinney KPW-4 vacuum system, capable of maintaining a vacuum better than  $10^{-3}$  torr, is used to evacuate the gun chamber. A 4-in. high-vacuum line extends from the diffusion pump to a point a few inches from the gun chamber. A pneumatically-operated, high-vacuum valve protects the diffusion pump from debris and exposure to atmospheric pressure. The fore pump is protected from all but very small particles by a fine wire screen located below the roughing line.

With the attachment shown in Figure 3, circular samples up to 7" in diameter and up to 3" thick can be tested. 3" x 3" samples with a 1" lip on each side can be tested in the stressed condition. Calibration of the attachment in the stressing mode is not complete yet, pending the acquisition of strain gauges.

## Shadowgraph Photography

Photographing small particles from the exploding-foil gun is complicated by the dense radiating plasma surrounding the

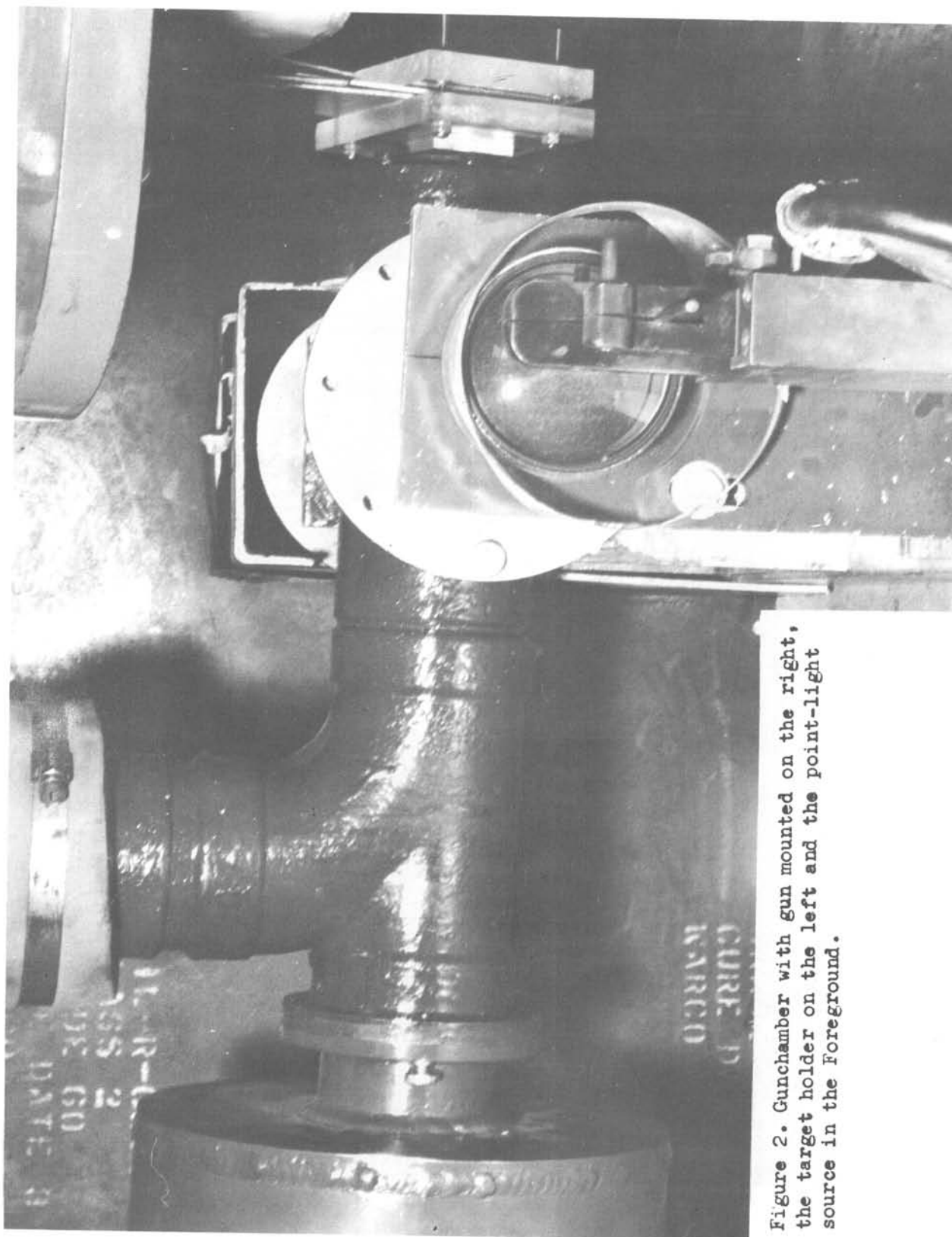


Figure 2. Gunchamber with gun mounted on the right, the target holder on the left and the point-light source in the Foreground.

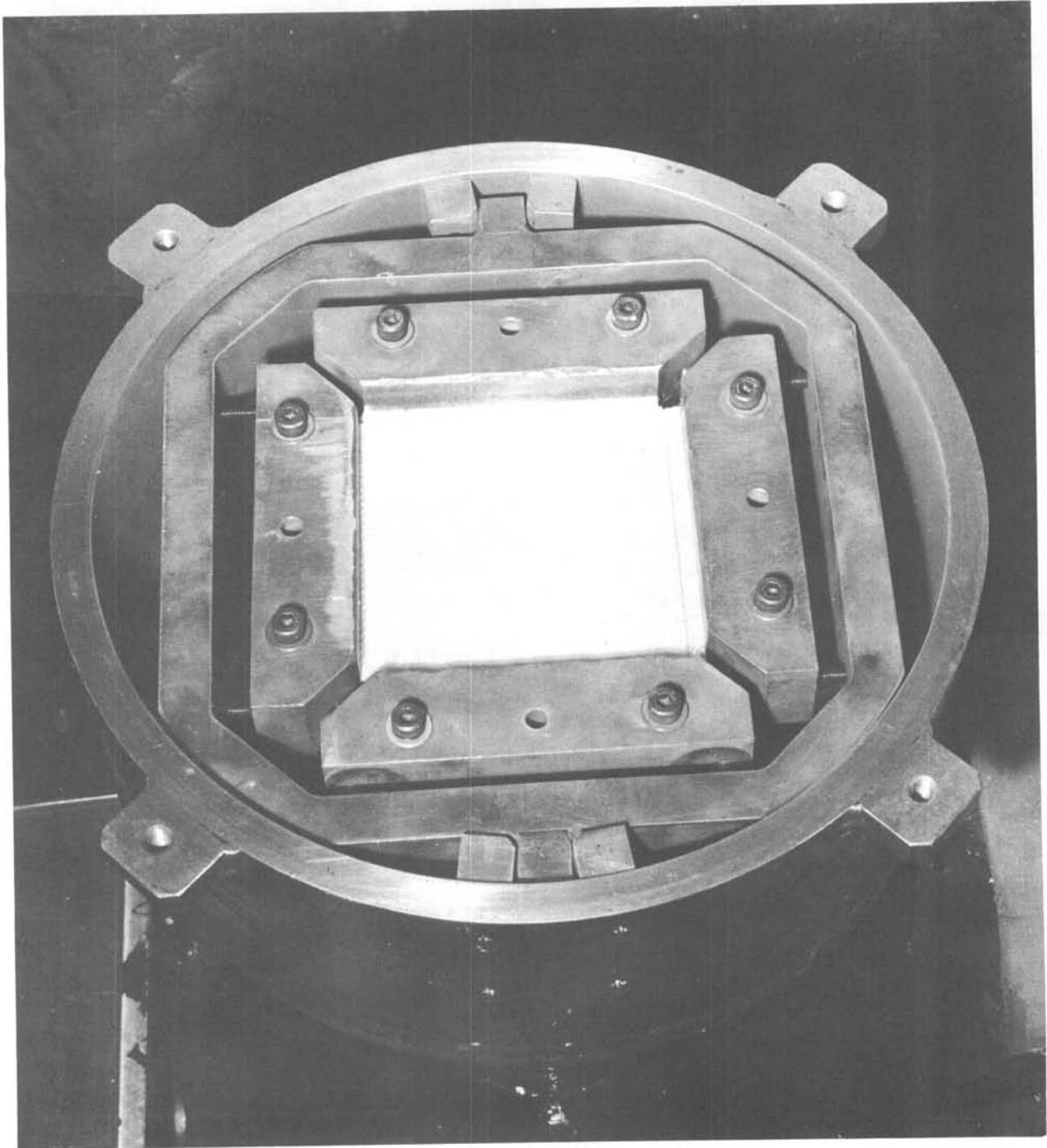


Figure 3. Target Holder. Shown is 3"x3" Target in Clamping Frame

particle in the free-flight region. We have found that we can discriminate against this plasma, however, by using an intense pulsed backlighting source to penetrate the plasma and illuminate the solid particle.

## Diagnostic Equipment

The diagnostic equipment associated with the AFML facility consists of a streak camera and a double-pulsed Kerr cell camera for determining particle in-flight parameters; a framing camera for target recoil studies; high intensity pulsed light source for shadowgraph photography; and high-speed oscilloscopes for measuring bank discharge characteristics and photomultiplier signals.

## Backlighting Sources

The high-intensity pulsed backlighting source was developed for use in the AFML facility. The unit, with a maximum stored energy of 7200 J, is used with a confined air arc. By proper choice of capacitance and inductance, the light pulse duration meets the requirements of the high-speed streak camera (15-30 $\mu$  sec.).

## Framing Camera

The Beckman & Whitley 339B camera is used in a unique way so as to allow for a framing as well as a streak record of the same event. Information on the particle shape and velocity can be obtained in this manner.

## Double-Pulsed Kerr Cell Camera

This camera uses a single Kerr cell shutter to take two pictures superimposed on the same film. The Kerr cell is

subjected to two voltage pulses with a variable time interval between pulses.

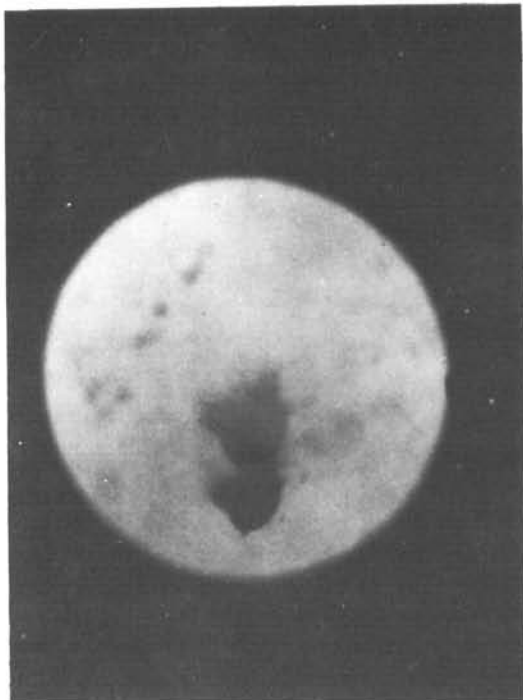
With this camera two 20-nsec exposures are obtained at precise interframe times of 1 through  $5\mu$  sec in  $1\mu$  sec steps. At the present we are using the same optical configuration for both cameras and using a beam splitter to divide the optics. In this manner we photograph the projectile from the same port with two different camera systems. Velocities measured by both cameras correlate to within 5%.

The Kerr-cell photographs in Figure 4 are an example of the information that can be obtained. The plasma surrounding the particle can be seen, as well as the poorly defined shape of the projectile itself. No. 570 shows a shattered particle.

#### DESCRIPTION OF OPERATION OF THE EXPLODING FOIL GUN

The gun is made up of three conductors electrically connected in series (Figure 5), with the one in the middle being the exploding aluminum foil. The electrical explosion is separated from the gun barrel and vacuum chamber by a mylar diaphragm (rupture disc) which confines the explosion for a short time interval during which the foil melts, vaporizes and begins to expand. In approximately  $2\mu$  sec. the diaphragm ruptures forming the disc-shaped particle. At the time of impact this particle weighs roughly 5 milligrams and travels at velocities between 7.5 and 9 kilometers per second. Single

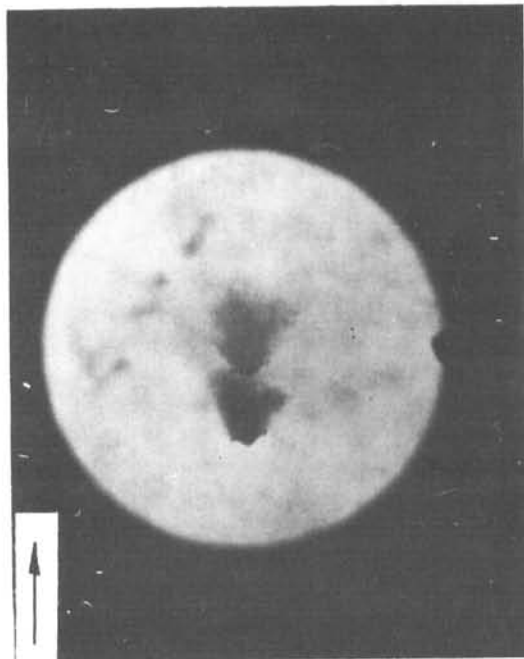




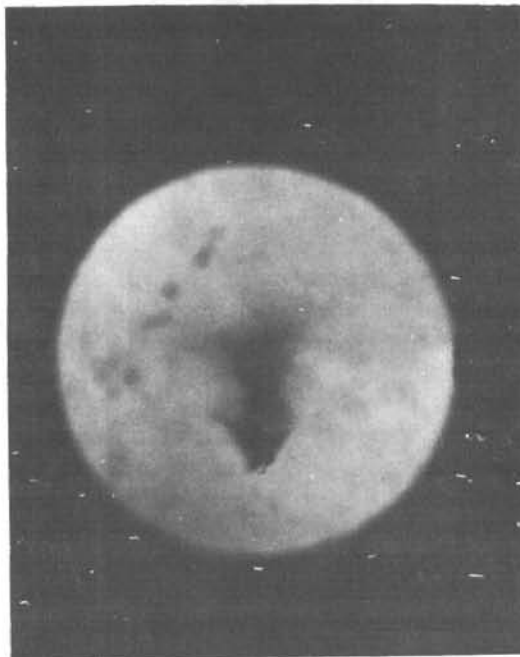
567



570



566



568

Figure 4. Examples of Double-pulsed Derr-cell Records. Arrow Indicates Direction of Travel

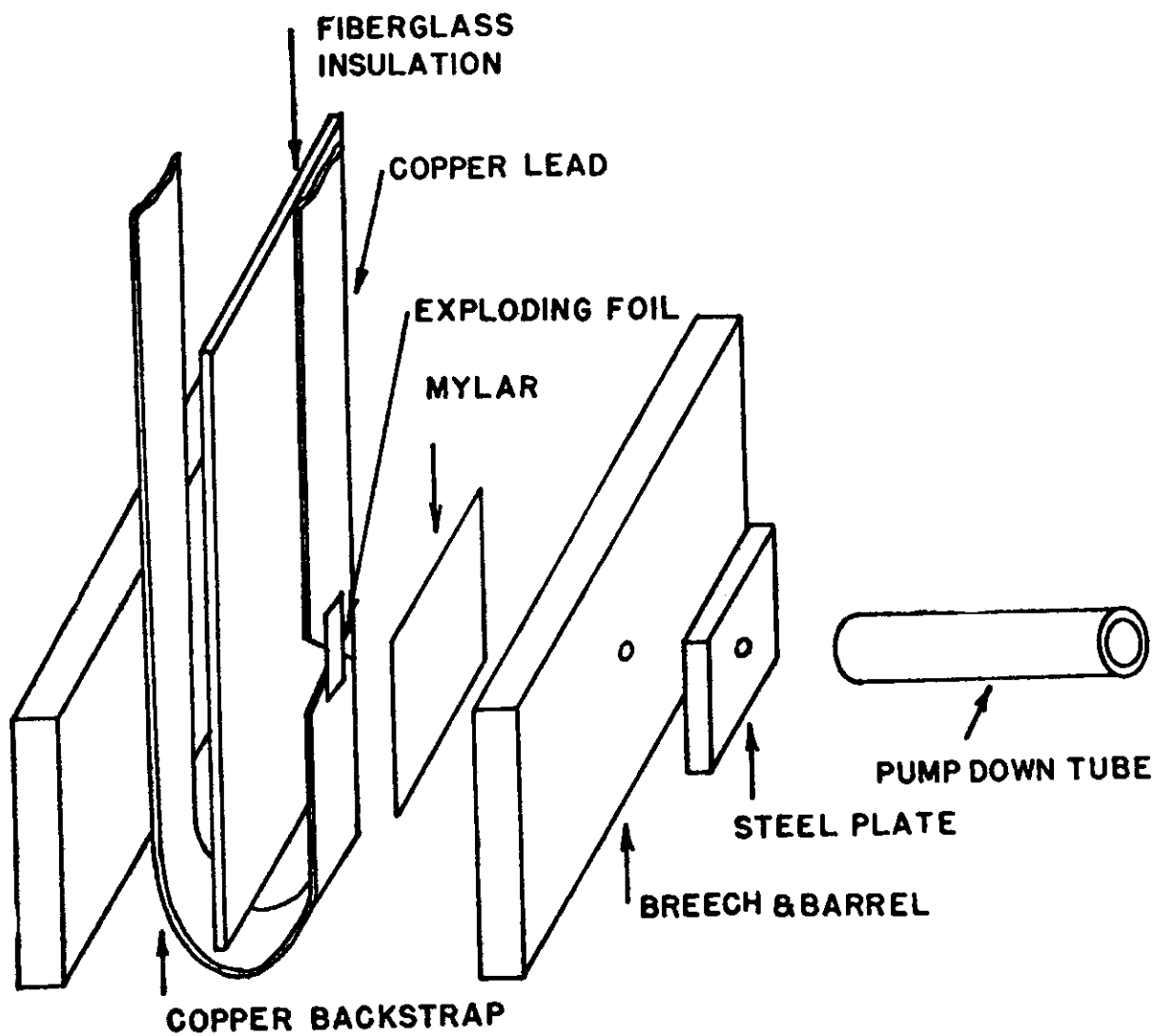


Figure 5. Exploding Foil Backstrap Gun

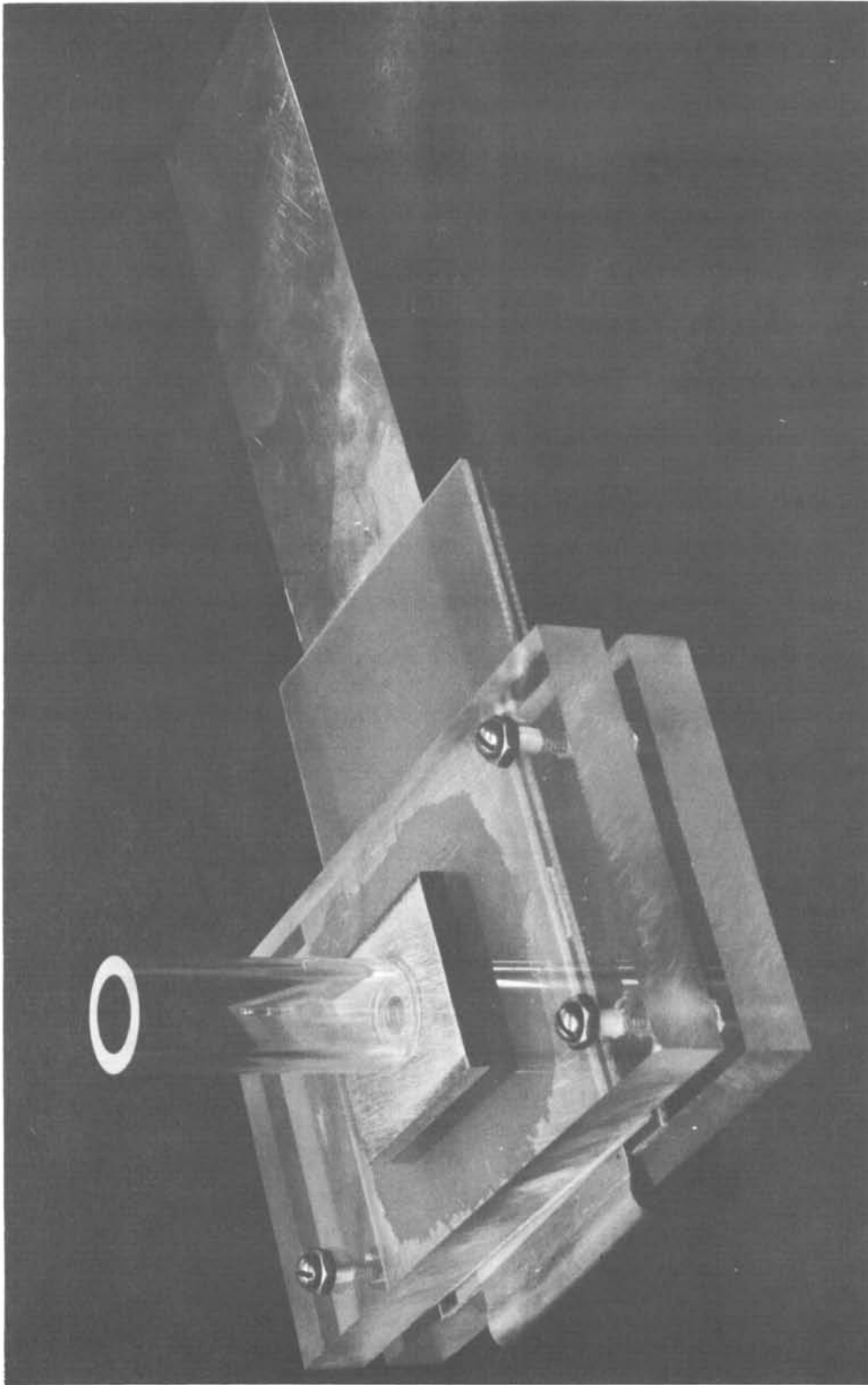


Figure 6. Exploding Foil Backstrap Gun

particle impacts at these velocities are achievable on approximately 50% of the shots fired, i.e. up to 5 impact data points per day. Figure 6 shows the gun in the assembled condition.

We are continuing the development of a gun that will enable us to accelerate spheres, between 50-100 $\mu$ in size, to speeds of around 20 kms. The gun designs studied include the coaxial gun, which has shown promise in free expansion studies conducted in the past, and the electrothermal gun, with which North American Aviation has been very successful.

### Projectile Mass Measurements

The projectile mass is determined from penetration equations. The use of these equations is valid because the data points or targets selected for mass determinations have nearly hemispherical craters (within 10%). The equation chosen was the following<sup>(2)</sup>

$$\frac{V_c}{V_p} = 0.12 \left( \frac{\rho_p}{\rho_t} \right)^{\frac{1}{2}} \left( \frac{\rho_p v^2}{S_T} \right)^{.845}$$

where

- $V_c$  = crater volume
- $V_p$  = projectile volume
- $\rho_p$  = projectile density
- $\rho_t$  = target density
- $v$  = velocity
- $S_T$  = target shear strength

Transposing this equation for mass calculations with lead targets one obtains:  $m_p = .63 \times \frac{V_c}{v^{1.69}}$  (v in Km/sec,  $V_c$  in  $cm^3$ ) We proceeded to calculate the projectile mass from selected single particle impacts which produced hemispherical craters. The projectiles in each case were Mylar  $\frac{1}{4}$ " diameter discs 0.010" thick having an initial weight of  $\sim 11$  mg. The average particle mass we obtained was 4.8 mg with a RMS error of 25%.

## TESTING OF EXPANDABLE STRUCTURES

The materials tested on the AFML facility are all described in more detail in other papers included in these proceedings. (3,4,5,6)

The Goodyear Aerospace specimens<sup>(3)</sup> were tested in the stressed as well as in the unstressed condition. With the 2" layer of 1 pcf foam the back surface was never damaged (Figure 7). It was then assumed that in certain applications the foam might be compressed to a fraction of its normal thickness (2 inches). In subsequent tests a typical 5 mg. mylar projectile travelling at 8 kms barely penetrated a sample compressed to 1" (rendering 2 pcf foam), while a similar particle travelling at a speed of 7.9 kms completely penetrated a sample compressed to  $\frac{1}{2}$  inch, i.e. 4 pcf foam (Figure 8).

The material developed by Whittaker Co.<sup>(4)</sup> showed similar effects. In the fully expanded state penetration was not possible, while in the compressed condition either serious damage or complete penetration of the back surface occurred (Figure 9). Since the dacron back surface is rigidized the damage observed usually was some form of spallation or delamination.

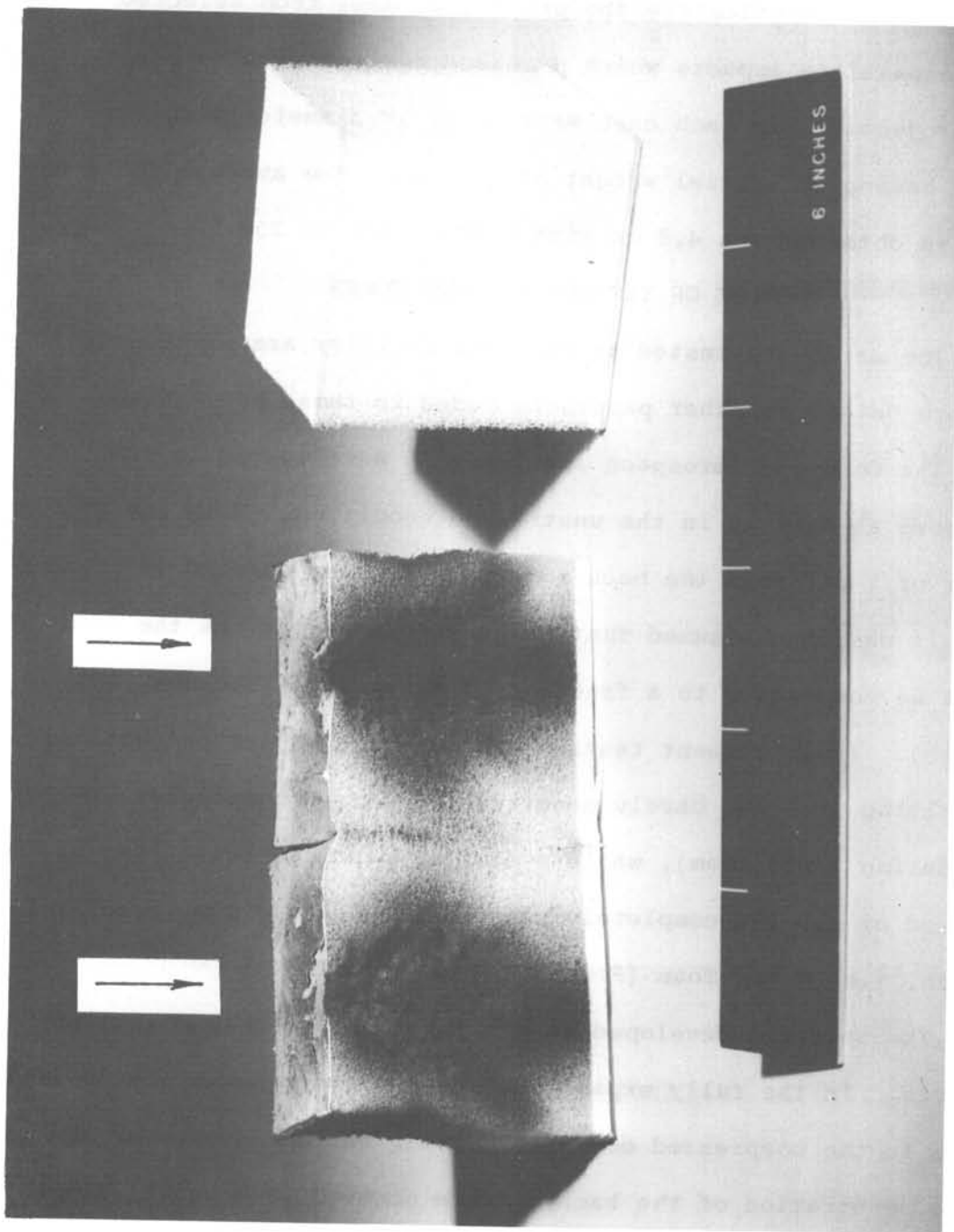


Figure 7. Goodyear Structure. Cutaway Shows Extent of Damage

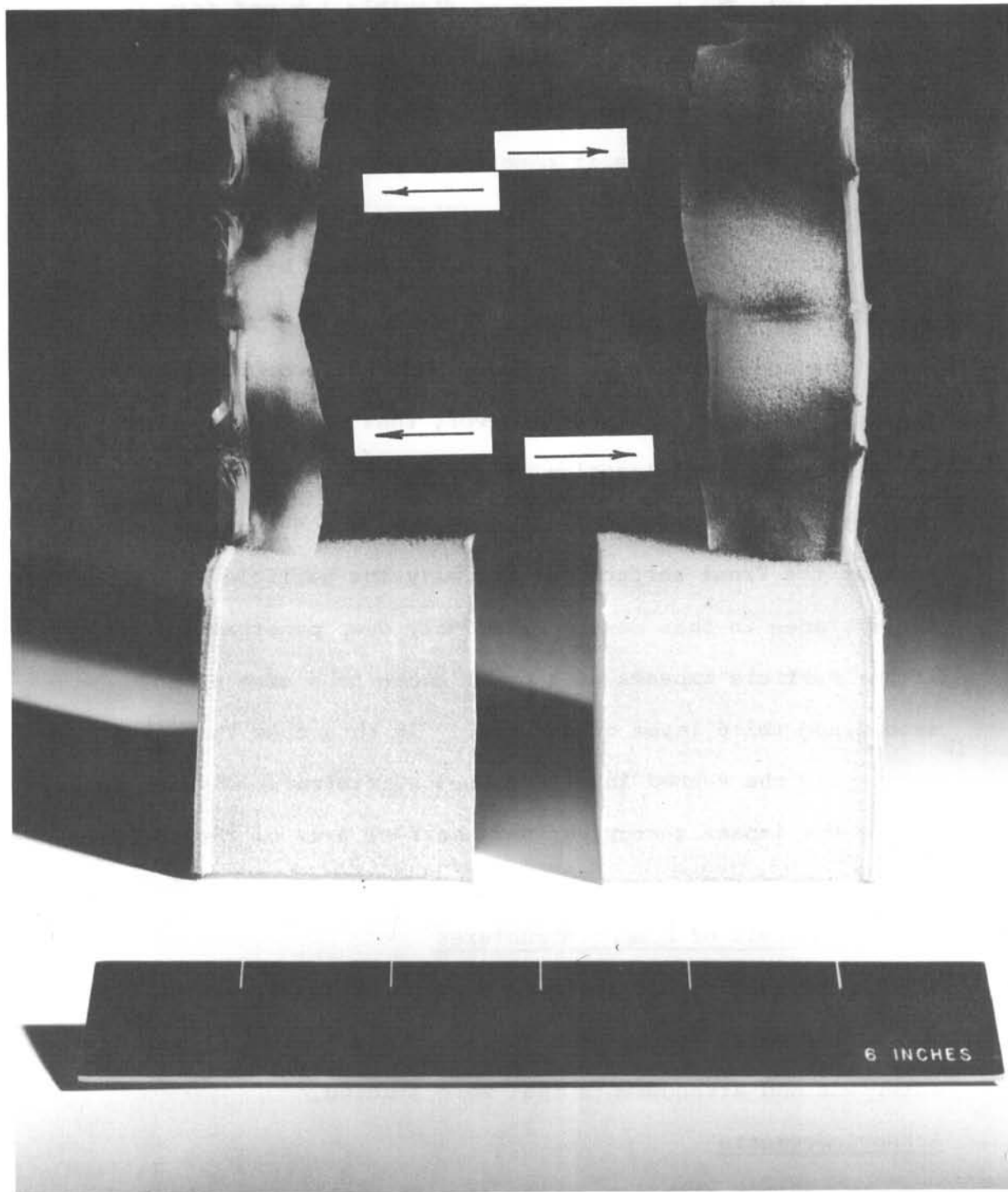


Figure 8. Goodyear Structure. Samples Compressed to 1/2" and 1".  
Arrows Indicate Direction of Particle Impact

Another material tested was that made by National Cash Register.<sup>(5)</sup> The  $\frac{1}{2}$  inch layer of flexible 1- $\frac{1}{2}$  pcf foam is backed by a layer of 15 pcf rigidized foam. A typical mylar projectile could not penetrate a specimen with a 1 inch layer of rigidized foam while it completely penetrated a sample with a  $\frac{1}{2}$  inch layer of rigidized foam (Figure 10).

A structure tested was the one developed by the Viron division of GCA.<sup>(6)</sup> The foams, used for each of the specimens impacted, differed. However, none were completely penetrated. It was discovered, however, that particle penetration was affected by the location of the point of impact (Figure 11). Deepest penetration was obtained if the impact occurred at a seam at the front surface; essentially the particle sees only two surfaces in this case. Relatively deep penetration occurs if the particle impacts at a point close to a seam of the second and third layer of material. In this case the spray created by the second layer does not sufficiently diverge to reduce the impact energy per unit surface area of the third layer.

### Ballistic Limit of Bumper Structures

Comparison studies were conducted looking at the ballistic limit of several bumper structures. Table I gives a list of the materials and arrangements that were studied.

### Acknowledgements

The author wishes to thank Alan K. Hopkins for his assistance in the preparation of this paper and John E. Myrberg for the preparation of the photographs.



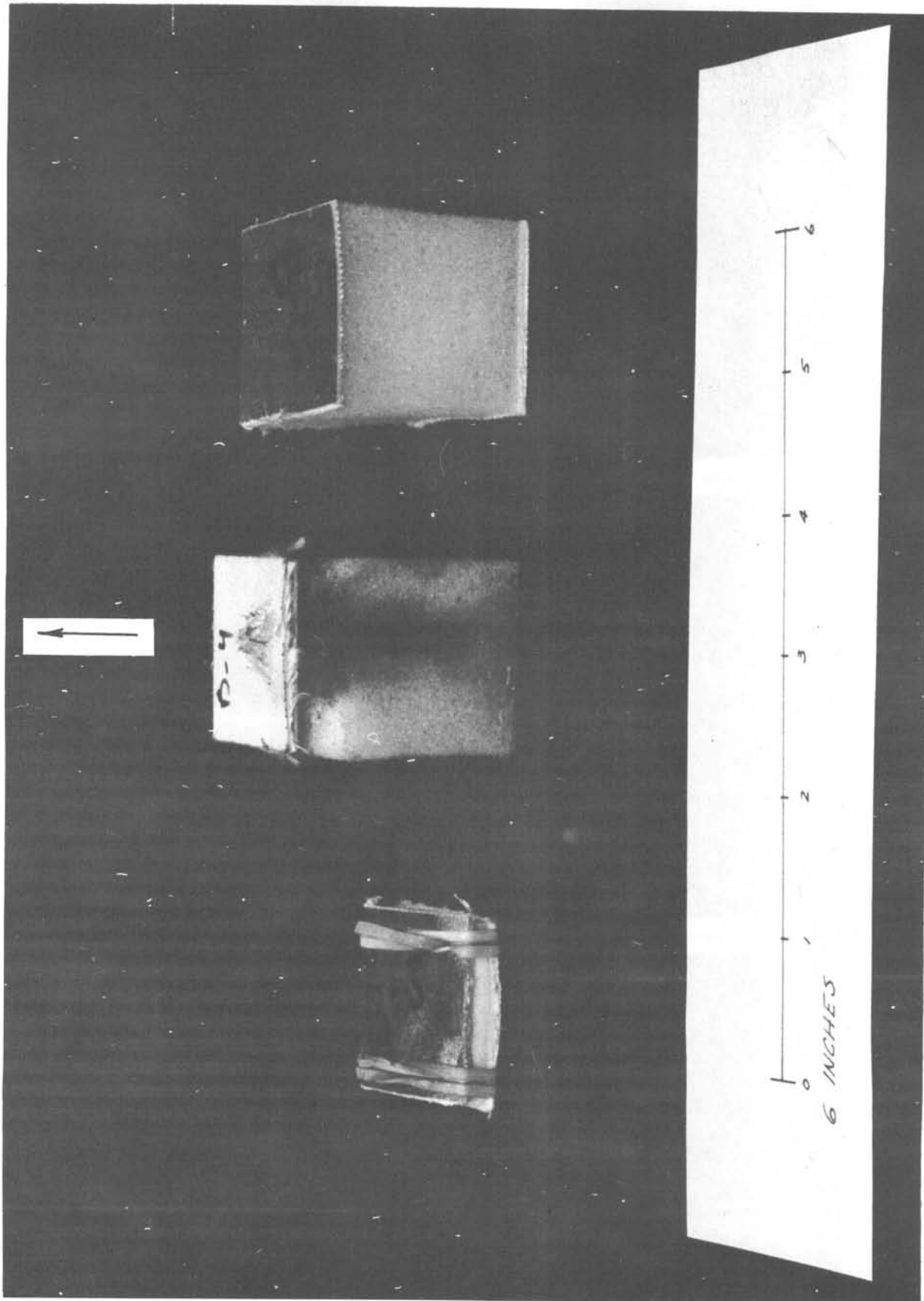


Figure 9. Whittaker Structure. Sample was Compressed as Shown on the Left. Damage to Back Surface can be seen on Sample in the Center

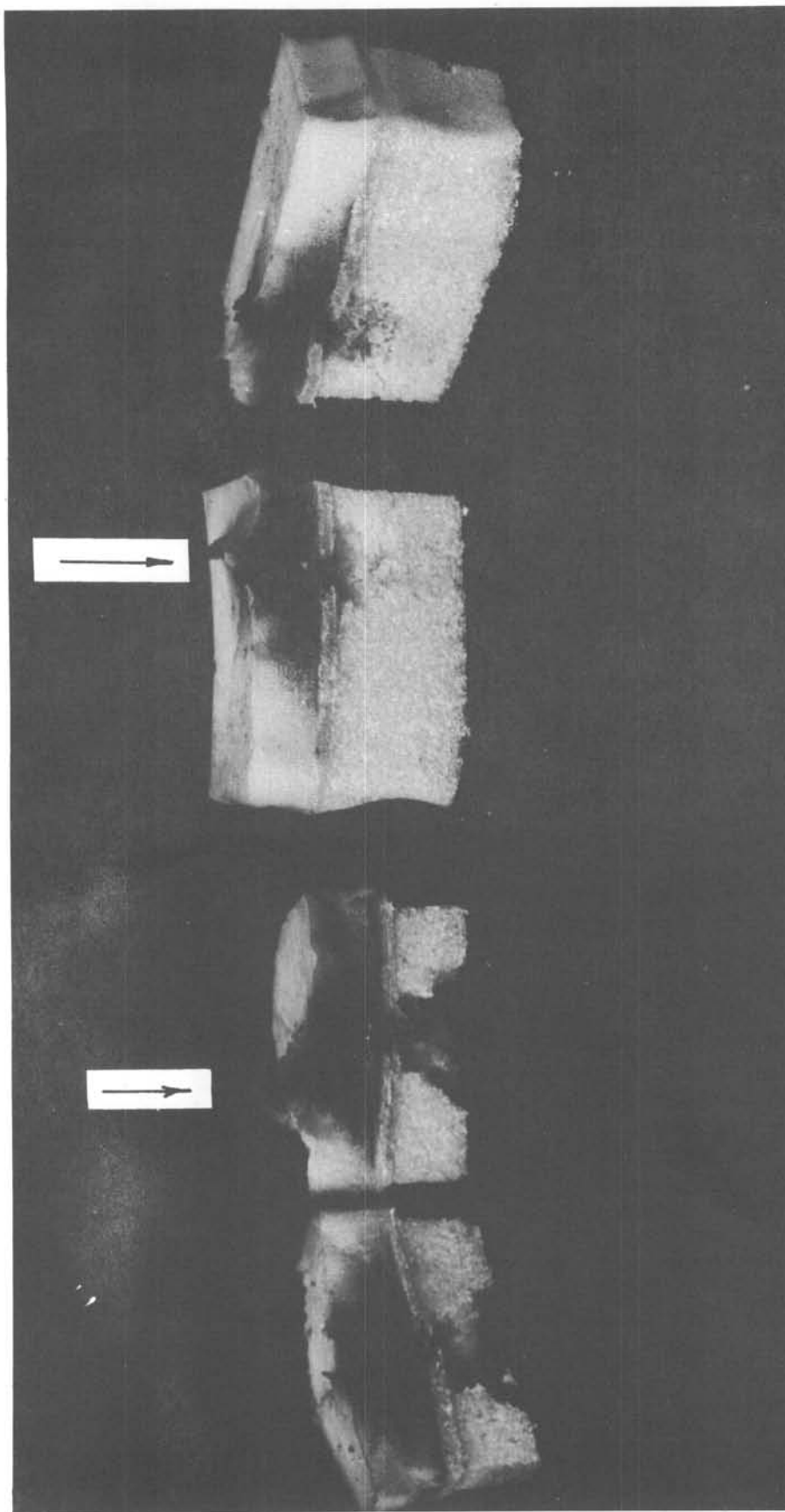


Figure 10. National Cash Register Structure. Samples have 1/2" (on the left) and 1" (on the right) Layer of Rigidized Foam

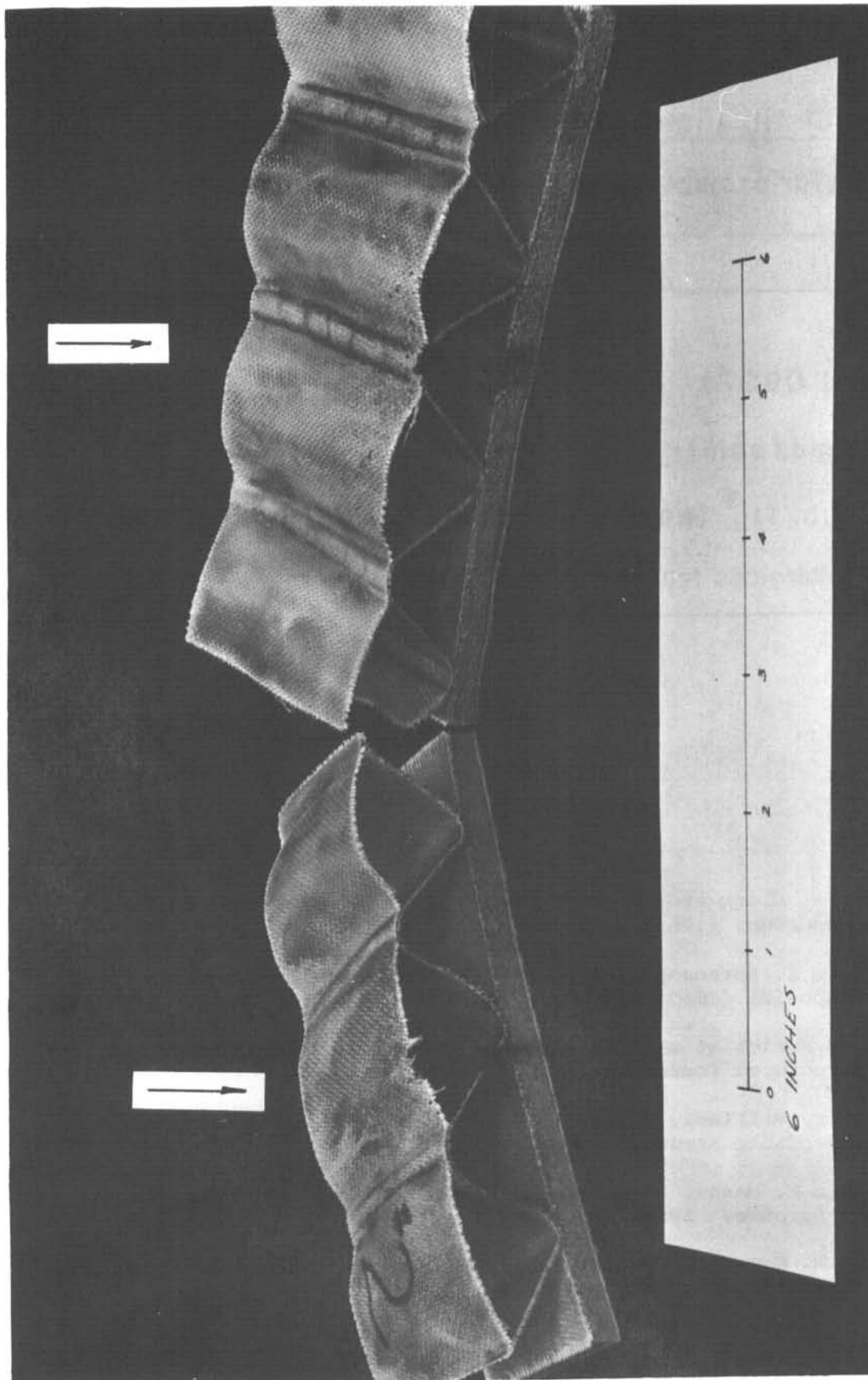


Figure 11. Viron-Geophysics Corp. of America Structure. Foam Type in Sample on the left is Vinyl (Firm, Closed Cell, 6.7 pcf) and in Sample on the right is Neoprene (Medium, Closed Cell, 18.3 pcf)

TABLE I

Ballistic Limit of Bumper Structures

for 5 mg mylar projectiles travelling between 7.5 and 9 kms.

Material	Total Thickness(inch)	Bal. Lim.(lb/ft <sup>2</sup> )
Al 2024 T3	1/4	3.60
Al (.010" and .090")	1	1.42
NCR(3/4" rigid.foam)	1 1/4	2.3
Goodyear (11b/ft <sup>3</sup> foam)	1 1/2	.60
GCA (.015" fiberglass truss)	1 1/4	.43

## REFERENCES

1. W. H. Clark et al. Proc of 7th Hypervelocity Impact Symposium. (1965) Vol. I - p. 207
2. Neil R. Sorenson. Proc. of 7th Hypervelocity Impact Symposium (1965) Vol. VI. - p. 281
3. Leo Jurich et al. Proc of 2nd Aerospace Expandable Structures Conference. 1965
4. Jerry Williams, Norman O. Brink. Proc of 2nd Aerospace Expandable Structures Conference. 1965
5. John F. Hanny. Proc of 2nd Aerospace Expandable Structures Conference. 1965
6. I. W. Russell, Charles Koons, Proc of 2nd Aerospace Expandable Structures Conference. 1965